EBioMedicine 69 (2021) 103471

Contents lists available at ScienceDirect

EBioMedicine

journal homepage: www.elsevier.com/locate/ebiom

Research Paper

Deciphering CT texture features of human visceral fat to evaluate metabolic disorders and surgery-induced weight loss effects

Juan Shi[a,1], Guoqing Bao[b,1], Jie Hong[a,1], Simin Wang[c], Yufei Chen[a], Shaoqian Zhao[a], Aibo Gao[a], Ru Zhang[d], Jingfen Hu[d], Wenjie Yang[c], Fuhua Yan[c], Ankang Lyu[e], Ruixin Liu[a], Bin Cui[a], Yuhong Chen[a], Jiabin Jin[f], Baiyong Shen[f], Yifei Zhang[a], Weiqiong Gu[a], Dagan Feng[g,h], Weiqing Wang[a], Jiqiu Wang[a,*], Xiuying Wang[b,*], Guang Ning[a,*]

[a] *Department of Endocrine and Metabolic Diseases, Shanghai Institute of Endocrine and Metabolic Diseases, Ruijin Hospital, Shanghai Jiao Tong University School of Medicine, Shanghai, China; Shanghai National Clinical Research Center for Metabolic Diseases, Key Laboratory for Endocrine and Metabolic Diseases of the National Health Commission of the PR China, Shanghai National Center for Translational Medicine, Ruijin Hospital, Shanghai Jiao Tong University School of Medicine, Shanghai, China*
[b] *School of Computer Science, The University of Sydney, Sydney, NSW, 2006, Australia*
[c] *Department of Radiology, Ruijin Hospital, Shanghai Jiao Tong University School of Medicine, Shanghai, China*
[d] *SAIC Volkswagen Automotive Company Limited, Shanghai, China*
[e] *Health Examination Centre, Department of Cardiology, Ruijin Hospital, Shanghai Jiao Tong University School of Medicine, Shanghai, China*
[f] *Department of General Surgery, Pancreatic Disease Center, Ruijin Hospital, Shanghai Jiao Tong University School of Medicine, Shanghai, China; Research Institute of Pancreatic Diseases, Shanghai Jiao Tong University School of Medicine, Shanghai, China*
[g] *SJTU-USYD Joint Research Alliance for Translational Medicine, Shanghai Jiao Tong University, Shanghai, China*
[h] *Biomedical and Multimedia Information Technology Research Group, School of Computer Science, The University of Sydney, Sydney, NSW 2006, Australia*

ARTICLE INFO

Article History:
Received 5 March 2021
Revised 12 June 2021
Accepted 15 June 2021
Available online xxx

Keywords:
Visceral fat
Texture feature
Bariatric surgery
Metabolic syndrome
Visceral obesity
Imaging biomarkers
Machine learning
Computer tomography

ABSTRACT

Background: Metabolic syndrome (MetS) is highly related to the excessive accumulation of visceral adipose tissue (VAT). Quantitative measurements of VAT are commonly applied in clinical practice for measurement of metabolic risks; however, it remains largely unknown whether the texture of VAT can evaluate visceral adiposity, stratify MetS and predict surgery-induced weight loss effects.
Methods: 675 Chinese adult volunteers and 63 obese patients (with bariatric surgery) were enrolled. Texture features were extracted from VATs of the computed tomography (CT) scans and machine learning was applied to identify significant imaging biomarkers associated with metabolic-related traits.
Findings: Combined with sex, ten VAT texture features achieved areas under the curve (AUCs) of 0.872, 0.888, 0.961, and 0.947 for predicting the prevalence of insulin resistance, MetS, central obesity, and visceral obesity, respectively. A novel imaging biomarker, RunEntropy, was identified to be significantly associated with major metabolic outcomes and a 3.5-year follow-up in 338 volunteers demonstrated its long-term effectiveness. More importantly, the preoperative imaging biomarkers yielded high AUCs and accuracies for estimation of surgery responses, including the percentage of excess weight loss (%EWL) (0.867 and 74.6%), postoperative BMI group (0.930 and 76.1%), postoperative insulin resistance (0.947 and 88.9%), and excess visceral fat loss (the proportion of visceral fat reduced over 50%; 0.928 and 84.1%).
Interpretation: This study shows that the texture features of VAT have significant clinical implications in evaluating metabolic disorders and predicting surgery-induced weight loss effects.
Funding: The complete list of funders can be found in the Acknowledgement section.

1. Introduction

Obesity is now a major public health problem and has become a pandemic [1]. The prevalence of obesity has risen globally from 3.2% to 10.8% in adult men and from 6.4% to 14.9% in adult women in the past several decades [2]. Obesity is usually determined by body mass index (BMI) and is strongly associated with a higher risk of type 2

* Corresponding authors.
E-mail addresses: wangjq@shsmu.edu.cn (J. Wang), xiu.wang@sydney.edu.au (X. Wang), gning@sibs.ac.cn (G. Ning).
[1] These authors contributed equally to this work.

https://doi.org/10.1016/j.ebiom.2021.103471

Research in context

Evidence before this study

Quantitative indices are applied for measuring adiposity in clinical practice. However, it remains largely unknown whether the qualitative factors, especially the texture of visceral adipose tissue (VAT), can be used to evaluate obesity-related traits, including metabolic syndrome (MetS) and the effectiveness of bariatric surgery. We searched PubMed using the medical terms "metabolic syndrome", "obesity", "visceral obesity", "visceral fat", "bariatric surgery" combined with "imaging features", "prediction" and "machine learning" up to October 1, 2020. We identified several studies for MetS estimation, none of which investigated the imaging texture features of visceral fat for estimation of MetS and prediction of weight loss effects of bariatric surgery.

Added value of this study

Texture biomarkers extracted from VAT and identified with machine learning achieved a high predictive power for estimating the prevalence of visceral obesity, MetS, as well as insulin resistance compared to body mass index, waist circumference, and visceral fat area. A novel imaging biomarker, *RunEntropy*, stratified voluntary participants into different risk groups with distinctive metabolic outcomes and demonstrated long-term effectiveness in follow-up studies. The preoperative imaging biomarkers yielded high performance for predicting postoperative outcomes, including the percentage of excess weight loss and postoperative BMI group, for 63 obese patients with bariatric surgery.

Implications of all the available evidence

VAT texture features could be served as new diagnostic indices for visceral obesity, insulin resistance as well as MetS, and preoperative predictors for the weight-loss effects of bariatric surgery. The novel imaging biomarkers, which can be obtained non-invasively in a low-radiation and economical manner, are applicable for clinical practice.

diabetes mellitus (T2DM), dyslipidemia, and cardiovascular diseases (CVD) [3,4]. However, BMI does not take into account the heterogeneity of body fat accumulation [5]. To better measure visceral obesity, waist circumference (WC) was adopted as a simple measurement for defining abdominal obesity [5], while WC was unable to distinguish subcutaneous (SAT) and visceral adipose tissue (VAT) [6].

A number of studies have generally reached a consensus that the accumulation of VAT is a key factor underlying obesity-related metabolic disorders, including insulin resistance, glucose intolerance, dyslipidemia, and elevated blood pressure [7–9]. This clustering of multiple metabolic abnormalities is referred to as "visceral fat syndrome" or "metabolic syndrome" (MetS). The hyperlipolytic state, chronic inflammation, endocrine function, and local fibrosis remodeling of VAT may partially explain the link between visceral obesity and MetS [7]. Thus, the characterization of VAT has become a hotspot for the investigation of obesity-related metabolic diseases in recent years.

Magnetic resonance imaging (MRI) and computer tomography (CT) are the gold-standard techniques for the quantitative measurement of VAT. A visceral fat area $\geq$ 100 cm^2 has been well accepted to define visceral obesity in the East Asian population [10]. In addition to quantitative assessment of visceral obesity, recent studies show that the qualities of different types of white adipose tissue (WAT) at the cellular level, such as adipocyte size [11], macrophage infiltration [12], angiogenesis [13], collagen production [14], extracellular fibrosis [15] and mitochondrial respiration [16], are associated with characteristics of different fat depots and corresponding metabolic and cardiovascular risks in obese subjects. In parallel with fat expansion, several molecular and pathomorphological changes [17], including apoptosis and new generation of adipocytes, branching of blood vessels and nerves, infiltration of various immune cells, and proliferation of fibrocytes remodel the texture of fat tissues, lead to a change in the sensitivity of adipocytes to insulin. The pathological expansion of WAT is usually considered as a major component or the main driver of MetS in obese individuals [18]. Unfortunately, in clinical practice, there is a lack of a direct and reliable approach to measure adipose tissue texture and quality for estimating its relationship with metabolic disorders until now.

As a novel image analysis technique, radiomics has been successfully applied to improve the diagnosis and prognostication of several cancers in recent years [19,20]. High-throughput texture features can be extracted from medical images with the technique. These imaging features are essentially 'hidden' in imaging big data and are usually not perceivable by the naked eyes [21]. However, such deep features may provide more and even better information to physicians for the prevention, diagnosis, or even treatment of diseases [22]. Recent studies demonstrated the discriminative abilities of quantitative and radiomic features constructed from abdominal regions for diagnosis of metabolic-related diseases. For example, Kim et al. measured areas of adipose tissues from abdominal CT scans and found deep subcutaneous adipose tissue is related to increased inflammation and oxidative stress, which could be served as a determinant of MetS [23]. Lu et al. constructed radiomic signatures from three abdominal organs of CT scans, and they found imaging features obtained from the pancreas showed higher discriminatory power for screening out early T2DM [24]. However, the role of the qualitative factors, especially the texture of visceral adipose tissue, in regarding to metabolic traits is largely unknown. Therefore, we attempted to measure the quality of fat tissues using high-throughput features. In addition, bariatric surgery provides an important option for effective weight loss, but the therapeutic response to surgery varies considerably among individuals [25]. Currently, the endeavor to address this variation in weight loss has proven to be less fruitful [26]. A hypothesis is thus raised in this study that the quality of VAT may have a close relationship with MetS and surgical response. To assess our hypothesis, metabolic-related imaging biomarkers obtained from VAT using various techniques, including fat segmentation, radiomics, and deep learning, were used to identify individuals at high risk of developing MetS in a Chinese population and estimate the weight loss response to bariatric surgery among obese subjects.

2. Methods

As shown in Fig 1, to investigate imaging biomarkers and their correlation with insulin resistance, MetS, central obesity, and visceral obesity, texture features of human visceral fat tissues were first measured, extracted, and analyzed. The potential associations between imaging biomarkers and other metabolic parameters, including visceral fat area, glucose, and lipid profiles, were further investigated. To evaluate the long-term effectiveness of the imaging biomarkers, a 3.5-year follow-up was conducted. Besides, the imaging biomarkers were applied to estimate the effectiveness of bariatric surgery.

2.1. Participants

A total of 693 workers from a deep phenotyping study of metabolic diseases at SAIC Volkswagen Automotive Company, Limited (Shanghai, China) were voluntarily recruited from December 2016 to January 2018 (denoted as MedSV cohort). All of them were young or

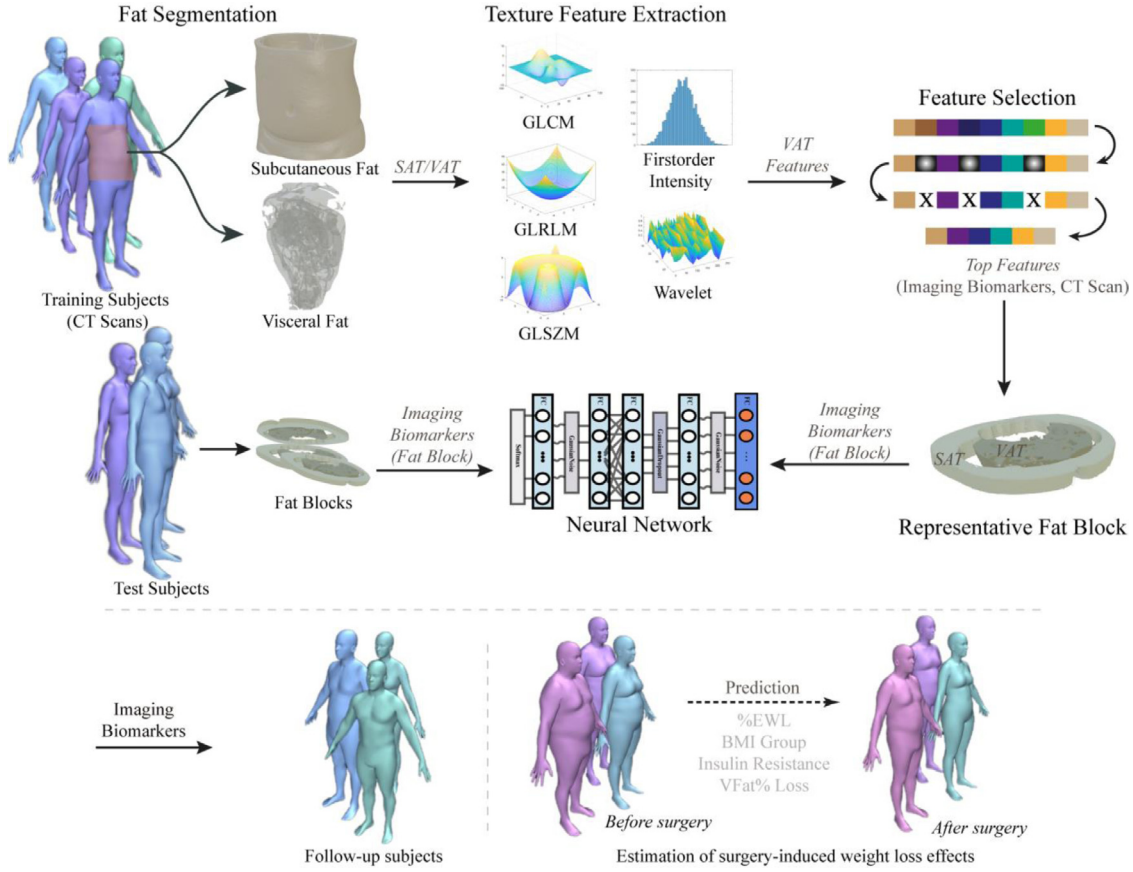

Fig. 1. Flowchart of the research design and methodology. The study cohort was arbitrarily separated into training/cross-validation (80%; n = 540) and testing (20%, n = 135) subjects (stratified according to MetS status). CT scans were segmented into SATs and VATs. Metabolic-related texture features[21] were extracted and identified from VATs of the training subjects (abdomen-pelvic CT scans). To be more clinically applicable, representative fat blocks instead of the entire CT scans were used. A feed-forward neural network was trained with metabolic-related imaging features extracted from representative fat blocks. The predictive power of the identified imaging biomarkers was evaluated on testing subjects. The effectiveness of the imaging biomarkers was further evaluated on population follow-up subjects and obese patients undergoing bariatric surgery (laparoscopic sleeve gastrectomy in this study).

middle-aged Han Chinese people (22 to 59 years old), among whom 675 volunteers with qualified CT images were ultimately included. Subjects who did not undergo non-contrast cardiac and non-contrast abdomen-pelvic CT scans or those without qualified image files were excluded from the analysis. The participants were followed up for MetS development with a median of 3.5 years and corresponding clinical information was re-collected during the follow-up. A long-term research project entitled "*Efficacy and Mechanism Study of Bariatric Surgery to Treat Moderate to Severe Obesity in Han Chinese Population*" was registered by this research team at ClinicalTrials.gov (No. NCT02653430) in January 2016, in which obese patients (BMI $\geq$ 35 kg/m^2 or BMI $\geq$ 32 kg/m^2 with at least one obesity complication) were enrolled in the specialized outpatient clinic for obesity treatment at Ruijin Hospital and underwent bariatric surgery after preoperative assessment. Patients with bariatric surgery routinely underwent both preoperative and postoperative upper-abdominal CT scans to obtain important outcome measures including abdominal fat deposition. A cohort consisting of 63 bariatric surgery studies with qualified preoperative and postoperative upper-abdominal CT images were involved in this observational research to explore the noninvasive method for preoperative evaluation of the surgery responses. The median follow-up interval for the bariatric surgery cohort is 13.0 months.

2.2. Ethics

The studies were approved by the Institutional Review Board of the Ruijin Hospital, Shanghai Jiao Tong University School of Medicine and were in accordance with the principle of the Helsinki Declaration (reference number: KY2016−75). Written informed consent was obtained from each participant.

2.3. Clinical data collection

Data collection was conducted at Ruijin Hospital by trained study personnel. A questionnaire including information on demographic characteristics, medical history, and lifestyle factors was administered by trained interviewers. Anthropometric measurements, including systolic blood pressure (SBP), diastolic blood pressure (DBP), height, weight, WC, and hip circumference (HC) were also collected for all participants. Blood pressures were measured at the 1-min interval after at least a 5-minute rest in the seated position. The measurements were repeated three times and mean values were adopted. The height and weight were measured with subjects in light clothes without shoes. Waist circumference (midway between the lower border of the rib cage and the top of the lateral border of the iliac crest) and hip circumference (the widest part over the greater trochanters) were measured at subjects' standing postures. BMI was calculated as weight in kilograms divided by height in meters squared and waist-to-hip ratio (WHR) was WC divided by HC.

Patients fasted overnight for at least 12 hours, and then, venous blood samples were collected. All participants (except 34 patients with a history of diabetes) finished a standard 75 g oral glucose tolerance test (OGTT). The 34 diabetic patients underwent a standard steamed bread meal test. Glycosylated hemoglobin (HbA1c) was measured by high-pressure liquid chromatography using the

VARIANT II Glycohemoglobin Testing System (Bio-Rad Laboratories, Hercules, CA, USA). High sensitivity C-reactive protein (hs-CRP) was measured by immunoprecipitation (Roche C311). Plasma glucose was measured by using the glucose oxidase method on an autoanalyzer (Beckman AU5800). Serum insulin concentrations were measured using an electrochemiluminescence immunoassay (ECLIA) on a Cobas e601 immunoassay analyzer (Roche Diagnostics). The insulin resistance index (homeostasis model assessment of insulin resistance, HOMA-IR) was defined as fasting insulin (IU/mL) × fasting glucose (mmol/L)/22.5

The CT examinations were performed on a dual-source CT scanner (SOMATOM Definition Flash, Siemens Healthcare). The scanner was calibrated before using both air and water phantoms. Each volunteer was examined in a supine position with both arms stretched above the head. A standard perspective ECG-gated (set to 30−80% of the R-R interval) scanning protocol was applied for the cardiac CT with 128 × 0.6-mm section collimation, 0.28-s gantry rotation time, and the pitch of 3.4. The tube current-time product and tube potential of all scans were selected automatically by CARE Dose4D and CARE kV (Siemens Healthcare, Forchheim, Germany) technology, respectively. The scan extended from the bifurcation of the pulmonary trunk to the diaphragm, including the whole heart. Another scanning protocol was applied for the abdomen-pelvic CT with 128 × 0.6-mm section collimation, 0.50-s gantry rotation time, the pitch of 0.6, and 120-kV tube voltage. CARE Dose4D technology was also used. The scan extended from the slice above the diaphragm to the last slice of the pelvic floor. Both of the cardiac and abdomen-pelvic scans were obtained during a single breath-hold.

2.4. Definition of metabolic-related traits

Overweight is defined as a BMI of 25.0−29.9 kg/m^2, and obesity is defined as a BMI of 30 kg/m^2 or above. Visceral fat area (VFA) was measured from both cross-sectional CT scans (umbilical level; named CT-VFA) using FatScan software (N2 Systems Inc.) [27] and Inbody device (InBody 720; named InBody-VFA). Subjects with a visceral fat area ≥ 100 cm^2 were defined as having visceral obesity according to the Asian criteria [10]. MetS is defined according to the U.S. National Cholesterol Education Program Adult Treatment Panel III (NCEP ATP III) guidelines [28] and modified as recommended in the latest American Heart Association/National Heart, Lung and Blood Institute Scientific Statement [29] by adopting the Asian criteria for waist circumference and a lower cutoff for fasting glucose levels. MetS is defined as meeting three or more of the following criteria: (1) central obesity (waist circumference ≥ 80 cm in females and ≥ 90 cm in males); (2) hypertriglyceridemia (fasting triglyceride ≥ 1.69 mmol/L); (3) low HDL cholesterol (fasting HDL-c < 1.29 mmol/L in females and < 1.04 mmol/L in males); 4) hyperglycemia (fasting glucose ≥ 5.6 mmol/L or taking hypoglycemic medications); and 5) hypertension (sitting blood pressure ≥ 130/85 mmHg or on regular antihypertensive medications). Insulin resistance was defined as HOMA-IR ≥ 2.5 [30]. The effectiveness of bariatric surgery was evaluated by the percentage of excess weight loss (%EWL), which was categorized into poor (%EWL < 50%), good (%EWL: 50% - 75%), and very good (%EWL ≥ 76%) [31]. %EWL was calculated as follows:

$$\%EWL = (W_i - W_a)/(W_i - W_d) * 100$$

where, W_i is initial weight (kg); W_a is actual weight (current weight (kg)); W_d is ideal weight (W_d = 24 × initial height (m) × initial height (m)) (31).

[2] GLCM: Gray Level Cooccurrence Matrix, GLRLM: Gray Level Run Length Matrix, GLSZM: Gray Level Size Zone Matrix

2.5. Extraction, identification, and evaluation of top imaging features from VAT

In-house software was designed to automatically detect the anatomical location of the diaphragm and pubic symphysis, and to separate VAT from SAT from the CT scan (denoted as whole-scan, illustrated in the upper-left panel, Fig 1). VAT and SAT volumes were calculated based on segmentation results. Five types of high-throughput texture features including *First Order Intensity, Gray Level Cooccurrence Matrix* (GLCM), *Gray Level Run Length Matrix* (GLRLM), *Gray Level Size Zone Matrix* (GLSZM), and *Wavelet* features were extracted from whole-scan VAT (upper-middle panel, Fig 1) using method proposed by van Griethuysen et al. [32]. A description of the meaning of each feature type can be found in the supplementary materials. The average Hounsfield unit, volume, and percentage of SAT and VAT (in account of total mass) were calculated by the software. The volunteer subjects were arbitrarily separated into 80% for training/cross-validation (n = 540) and the remaining 20% for testing (n = 135). The separation was stratified by MetS status. The top ten texture features were selected as imaging biomarkers for carrying out the following studies based on their Gini Index [33] in the whole-scan training subjects (upper-right panel, Fig 1).

In considering the sample size and the number of input features, a nine-layer neural network model consisting of five fully connected layers (with nodes of 1024, 512, 256, 128, and 64, respectively), two Gaussian noise layers, one Gaussian dropout layer, and a Softmax layer was proposed in this study to estimate the performance of selected imaging biomarkers (middle panel, Fig 1). The noise and dropout layers served to improve the generalization of the neural network by introducing input variances and reducing dependences within neurons. L2 regularization that restrains the network weights and biases was utilized to reduce overfitting. He-normalization [34] was adopted to initialize network weights. A hyperparameter search was conducted under 10-fold stratified cross-validation using whole-scan training subjects. The performance of the proposed network model was compared with traditional machine learning methods, i.e., Random Forests (RF) and Support Vector Machine (SVM). RF model contains 100 trees with a minimum of 1 sample leaf; Gini impurity was used to measure the quality of a split. In SVM, RBF kernel with regularization C of 1.0 and degree of the polynomial kernel function of 3 was used.

The whole CT scan of each MedSV subject from the diaphragm to pubic symphysis was divided into ten equal CT blocks to explore low-radiation and cost-effective approaches suitable for clinical practice. The number of CT slices in a block is dependent on the voxel size, which is on average of ~51 slices per block or ~51 mm thick. The imaging biomarkers obtained from whole-scan training subjects were also extracted from each CT block. The representative CT block (middle-right panel, Fig 1) was identified by comparing the overall cross-validation performance of imaging biomarkers extracted from different fat blocks. The performance was measured by accuracy, precision, recall, f1-score, and area under the receiver operating characteristic curve (ROC/AUC). The imaging biomarkers obtained from the representative CT block, which achieved the highest cross-validation performance, were used to carry out the following analyses. Testing subjects were further used to evaluate their performances (middle-left panel, Fig 1). The identified imaging biomarkers were further extracted from CT images of obese subjects before and after bariatric surgery.

2.6. Association of imaging biomarkers with clinical parameters

Hierarchical clustering of imaging biomarkers with a distance based on the Pearson correlation coefficient was performed. The clustering result was presented as a heatmap that illustrates the relationship between clinical parameters and the pattern of the imaging

biomarkers. The volunteer subjects were stratified into different subgroups using the median values of clinical factors and imaging biomarkers for correlation analysis. The Sankey diagram was used to show the relationship between those subgroups. The most significant imaging biomarker and its correlation with clinical factors were specifically analyzed with Mosaic Display, in which the volunteer subjects were stratified into four subgroups (Low, Medium-Low, Medium-High, and High) based on the mean and two standard deviations of the imaging biomarker. For each subgroup, the distribution of the clinical factors or metabolic outcomes was calculated. Similarly, the relationship between the imaging biomarker and other factors including age, sex, and the volume of SAT and VAT (SFat, VFat), were also analyzed.

2.7. Statistical analysis

Statistical analyses including linear and logistic regression, Students' *t*-test, Chi-square test, and one-way ANOVA were performed with SPSS version 19.0 (Chicago, IL, USA), Python 3.6 (https://www.python.org/) for Sankey diagram, and R 3.5.1 (https://www.r-project.org/) for z-score normalization, hierarchical clustering, and Pearson's correlation analyses. Data were tested for normal distribution and logarithmically transformed for statistical analysis when required. Baseline characteristics according to overweight/obese status were presented as proportions or median (interquartile range). The Students' *t*-test was used to compare continuous variables and Chi-square tests for categorical variables between the normal-weight and overweight/obese groups. Paired Students' *t*-test was used to compare biomarkers before and after bariatric surgery. One-way ANOVA was used to compare continuous variables across quartiles of *RunEntropy*. Correlations were calculated by Spearman correlation coefficients. HOMA-IR was regressed on the *RunEntropy* with adjustment for covariates, including age, sex, BMI, and CT-VFA. Receiver operating characteristic (ROC) curve analyses were performed to assess the predictive power of identified imaging biomarkers for determining the prevalence of MetS, insulin resistance, central obesity, and visceral obesity. Imaging feature data were scaled by z-score and subjected to hierarchical clustering (with Pearson's correlation distance) to find patterns related to clinical factors and/or major metabolic outcomes. For surgery studies, multinomial logistic regression analyses were conducted with preoperative imaging biomarkers as covariates (bottom-right panel, Fig 1) and postoperative outcomes, e.g., %EWL category, postoperative BMI group, and postoperative insulin resistance, as target variables. Age, sex, fat area, and fat percentage were also involved as covariates to test whether these conventional parameters can boost the predictive performance of the texture imaging biomarkers.

2.8. Role of the funding source

The funder had no role in study design, data collection, data analysis, data interpretation, or writing of the report. The corresponding authors had full access to all the data in the study and had final responsibility for the decision to submit it for publication.

3. Results

3.1. Clinical characteristics of participants

In the MedSV cohort, 40.6% of participants (n = 274) were subjects with normal weight (BMI $<$ 25.0 kg/m^2), and 59.4% (n = 401) were overweight or obese (BMI $\geq$ 25.0 kg/m^2). As expected, the overweight/obese group showed a higher prevalence of MetS than the normal weight group (Chi-square test, $P < 0.001$) (Table 1). Besides, almost all metabolic risk factors, including BMI, WC, blood pressure, total cholesterol (TC), triglycerides (TG), LDL cholesterol (LDL-c), fasting plasma glucose (FPG), 2-h plasma glucose (2-h PG), and HOMA-IR, were significantly higher in the overweight/obese group (Students' *t*-test, all $P < 0.001$), whereas the serum HDL-c levels were lower (Students' *t*-test, $P < 0.001$). Of note, the overweight/obese group showed much higher fat content of both VAT and SAT measured by fat area or volume (Students' *t*-test, all $P < 0.001$) (Table 1).

Table 1
Baseline characteristics of MedSV cohort.

Characteristics	Normal weight (n = 274)	Overweight/Obese (n = 401)	P-value
Age (yrs)	34.0 (28.0–43.3)	34.0 (29.0–41.0)	0.497
Men (%)	61.7	90.3	< 0.001
BMI (kg/m^2)	22.15 (20.69–23.62)	30.24 (27.54–32.37)	< 0.001
Waist circumference (cm)	81.00 (75.00–85.75)	101.90 (94.70–107.50)	< 0.001
Systolic blood pressure (mmHg)	116.0 (109.0–124.0)	127.0 (120.5–135.5)	< 0.001
Diastolic blood pressure (mmHg)	75.0 (68.0–81.0)	80.5 (74.5–87.5)	< 0.001
Fasting plasma glucose (mmol/L)	5.24 (4.98–5.55)	5.50 (5.19–5.98)	< 0.001
2-h plasma glucose (mmol/L)	5.60 (4.90–6.49)	6.45 (5.35–7.76)	< 0.001
Fasting serum insulin (uIU/L)	8.00 (5.71–10.77)	13.70 (10.60–20.03)	< 0.001
2-h serum insulin (uIU/L)	37.20 (23.12–55.55)	64.70 (36.95–106.58)	< 0.001
HbA1c (%)	5.30 (5.10–5.50)	5.40 (5.20–5.75)	< 0.001
HOMA-IR	1.91 (1.31–2.70)	3.51 (2.55–5.18)	< 0.001
hs-CRP (mg/L)	0.46 (0.30–0.82)	1.04 (0.54–2.07)	< 0.001
Total cholesterol (mmol/L)	4.96 (4.34–5.63)	5.13 (4.53–5.88)	0.004
Triglycerides (mmol/L)	1.02 (0.73–1.46)	1.65 (1.19–2.43)	< 0.001
HDL cholesterol (mmol/L)	1.50 (1.23–1.75)	1.16 (1.01–1.32)	< 0.001
LDL cholesterol (mmol/L)	2.90 (2.42–3.50)	3.26 (2.73–3.87)	< 0.001
Subcutaneous fat area-CT (cm^2)	141.55 (105.48–172.10)	285.30 (226.48–356.75)	< 0.001
Visceral fat area-CT (cm^2)	90.55 (62.98–123.03)	174.55 (141.58–208.48)	< 0.001
Visceral fat area-Inbody (cm^2)	74.40 (58.30–91.20)	127.65 (109.83–144.65)	< 0.001
Subcutaneous fat volume (L)	4.11 (3.21–5.19)	8.45 (6.31–10.83)	< 0.001
Visceral fat volume (L)	1.60 (0.89–2.55)	4.28 (3.30–5.24)	< 0.001
MetS (%)	12.8	57.4	< 0.001

Data are given as median (interquartile range) or the percentage.

3.2. Imaging biomarkers identified from VAT for diagnosis of metabolic disorders

To non-invasively estimate the metabolic-related disorders, a total of 377 high-throughput features were extracted from VATs in abdomen-pelvic CT scans (whole-scans). By correlating with MetS status, the top ten features obtained from whole-scan training subjects were selected as metabolic-related imaging biomarkers. Among the CT blocks, imaging biomarkers extracted around the umbilicus level achieved the best performance in comparison with other blocks (CT positions) as well as the entire CT scan under cross-validation (S1 Table).

In combination with sex as a covariate, the neural network model was trained with the ten metabolic-related imaging biomarkers that were extracted from umbilicus blocks of the training subjects. The age factor was not involved at this stage since it did not induce a significant performance boost under cross-validation. The trained models were finally evaluated on the corresponding testing subjects. The metabolic-related imaging biomarkers demonstrated high AUCs and

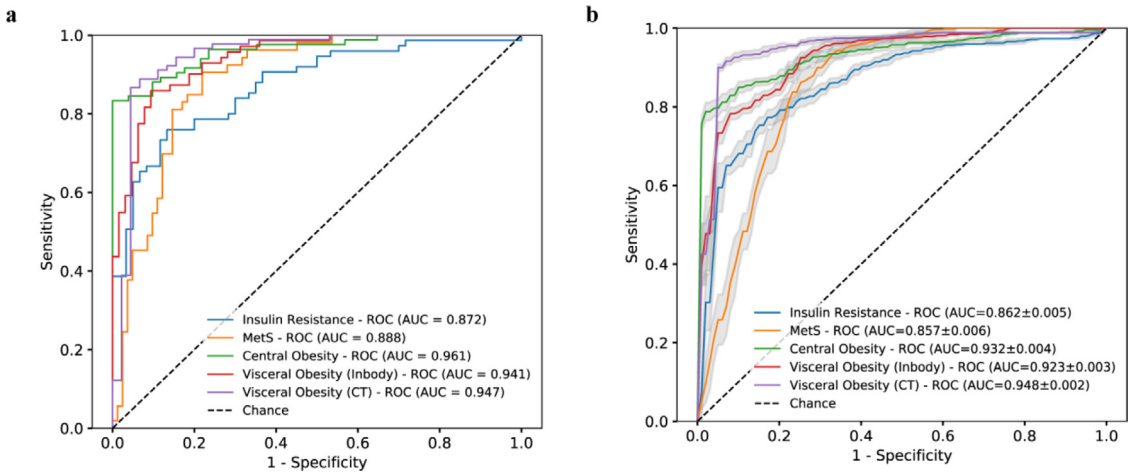

Fig. 2. ROC/AUCs of imaging biomarkers for assessment of metabolic-related traits on testing samples (n = 135). Imaging biomarkers extracted from umbilicus block (a) and slices (b).

accuracies for predicting the prevalence of insulin resistance (0.872, 77.0%), MetS (0.888, 83.0%), central obesity (0.961, 88.9%), and visceral obesity (0.941 and 85.9% against Inbody-VFA; 0.947 and 91.1% against CT-VFA/FatScan, respectively) (Fig 2a and Table 2). The neural network proposed in this study achieved better overall test performance compared to traditional machine learning methods, i.e., RF and SVM (S2 Table). For instance, MetS with neural network achieved AUC and accuracy of 0.888 and 83.0% respectively in comparison to RF (0.864 and 75.6%) and SVM (0.861 and 80.0%).

The imaging biomarkers were further extracted from any three consecutive CT slices within the umbilicus block (10 times at random positions), and the experimental results demonstrated the predictive robustness of texture features obtained around the umbilicus level, which was a slightly lower but comparable performance compared to features obtained from the whole umbilicus block (Fig 2b and S3 Table). Imaging biomarkers from both the umbilicus block and slices yielded consistent results for the diagnosis of visceral obesity especially against the FatScan method compared to the InBody device, which indicated that our method could serve as an alternative measurement strategy.

3.3. Correlation between imaging biomarkers and clinical outcomes

Hierarchical clustering exhibited distinctive patterns of the imaging biomarkers in relation to MetS, visceral obesity, and insulin resistance (Fig 3). The heatmap indicated that the metabolic-related imaging biomarkers, as imaging signature, can effectively stratify MetS, visceral obesity, and insulin resistance cases from subjects without these disorders. The signature was more closely related to visceral than subcutaneous fat volume. A similar correlation pattern was also found in the heatmap with clustering of all high-throughput features (S1 Fig).

As shown in Fig 4, the relationship among visceral fat volumes (left panel), metabolic outcomes (right panel), and the top four imaging biomarkers obtained from the umbilicus block (middle panel), i.e., wavelet-HHH GLRLM_RunEntropy (*RunEntropy* for short in this study), GLSZM_GrayLevelVariance (*GrayLevelVariance*), wavelet-LLH glcm_Id (*glcm_Id*), and wavelet-LLH glcm_Idm (*glcm_Idm*) were disclosed and visualized as a Sankey diagram. Each of the four biomarkers was divided into high (H) and low (L) based on their median values.

Table 2
Test performance metrics of neural network using identified imaging biomarkers extracted from umbilicus block.

Metabolic Traits	Precision	F1-score	Accuracy	AUC
Insulin Resistance	0.771	0.768	0.770	0.872
MetS	0.834	0.831	0.830	0.888
Central Obesity	0.893	0.890	0.889	0.961
Visceral Obesity (Inbody)	0.861	0.859	0.859	0.941
Visceral Obesity (CT)	0.912	0.909	0.911	0.947

Note: Recall is not shown here since it is the same as accuracy results in the weighted-average calculation in this work.

The diagram shows that most subjects with HHLL characteristics, which indicate high *RunEntropy* and *GrayLevelVariance*, and low *glcm_Id* and *glcm_Idm*, have high visceral fat volumes and a high prevalence rate of insulin resistance, whereas subjects with the LLHH phenotype, which denotes low *RunEntropy* and *GrayLevelVariance*, and high *glcm_Id* and *glcm_Idm*, have low visceral fat volumes and a low prevalence rate of MetS. Of note, these imaging biomarkers were significantly different in subjects with and without metabolic disorders (Students' t-test, all $P < 0.0001$, Table 3). The imaging biomarkers were also related to Non-alcoholic fatty liver disease (NAFLD) (S4 Table) and T2DM (S5 Table).

In general, subjects with HHLL biomarker carriers demonstrate a high risk of developing insulin resistance, whereas LLHH characteristics are more useful for screening non-MetS subjects. The meanings of the abovementioned features are summarized in S1 Definition in the supplementary materials. Briefly, *RunEntropy* and *GrayLevelVariance* measure heterogeneity, and *glcm_Id* and *glcm_Idm* measure the homogeneity of the specific CT image area.

3.4. A novel imaging biomarker RunEntropy that related to metabolic-related traits

Based on the mean and two standard deviations of *RunEntropy*, the volunteer subjects were stratified into four *RunEntropy* subgroups: Low (< 2.7, n = 171), Medium-Low (≥ 2.7 & < 2.79, n = 164), Medium-High (≥ 2.79 & < 2.95, n = 175) and High (≥ 2.95, n = 165). The increased value of *RunEntropy* was found to be significantly associated with an increased prevalence of metabolic disorders (Fig 5); for example, the *High-RunEntropy* subgroup demonstrated a significantly higher (Chi-square test, $P < 0.001$) prevalence rate of MetS and insulin resistance (73.3% and 90.9%, respectively) than the *Low-RunEntropy* subgroup (5.8% and 19.3%, respectively) (Fig 5a,b). Similar patterns were also found for central obesity and visceral obesity, in which the *High-RunEntropy* subgroup demonstrated a very high prevalence rate (over 99% for both central obesity and visceral obesity) compared to the *Low-RunEntropy* group (14.6% and 17%, respectively) (Fig 5c,d). Furthermore, the subjects with high *RunEntropy* tended to have excessive subcutaneous and visceral fat volume compared to

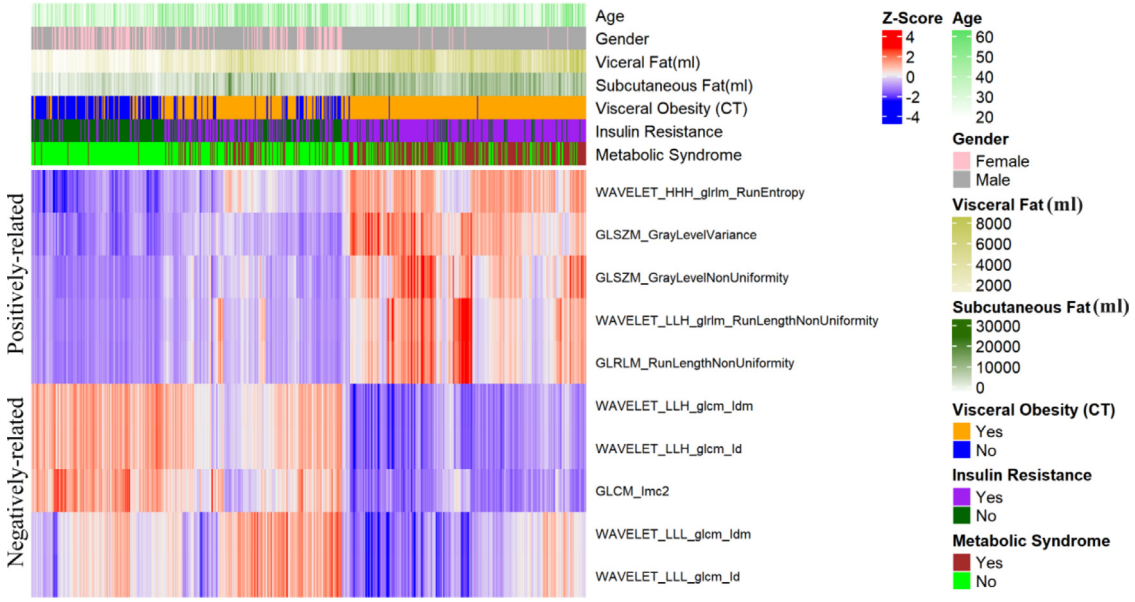

Fig. 3. Hierarchical clustering of metabolic-related imaging biomarkers. Imaging features positively (up) and negatively correlated (down) with clinical parameters and metabolic traits. Z-score is calculated by subtracting the population mean of raw values and dividing the standard deviation.

those with low *RunEntropy* (Fig 5e,f). The imaging biomarker was more closely associated with visceral fat volume than subcutaneous fat volume (Fig 5e,f).

Both age and sex were closely associated with the imaging biomarker (Fig 6a,b). The risk for developing MetS increased accordingly with increasing age, especially for subjects over 42 years old in the *Medium-* and *High-RunEntropy* subgroups (Fig 6b). Despite a similarly low risk for both female and male subjects in the *Low-RunEntropy* subgroup, a higher risk was found in male cases with higher *RunEntropy* (Fig 6a). As expected, subjects diagnosed with visceral obesity by CT scan had a higher risk of developing MetS and insulin resistance than their normal counterparts (Fig 6c,d).

We further found that this imaging biomarker alone achieved superior performances for the diagnosis of MetS (AUC of 0.819, 95% CI: 0.79−0.85) and insulin resistance (AUC of 0.816, 95% CI: 0.78−0.85), compared to BMI and WC, and similar performance with VFA (CT-VFA) (Fig 7a,b), while the measurement of *RunEntropy* biomarker is much easier than CT-VFA.

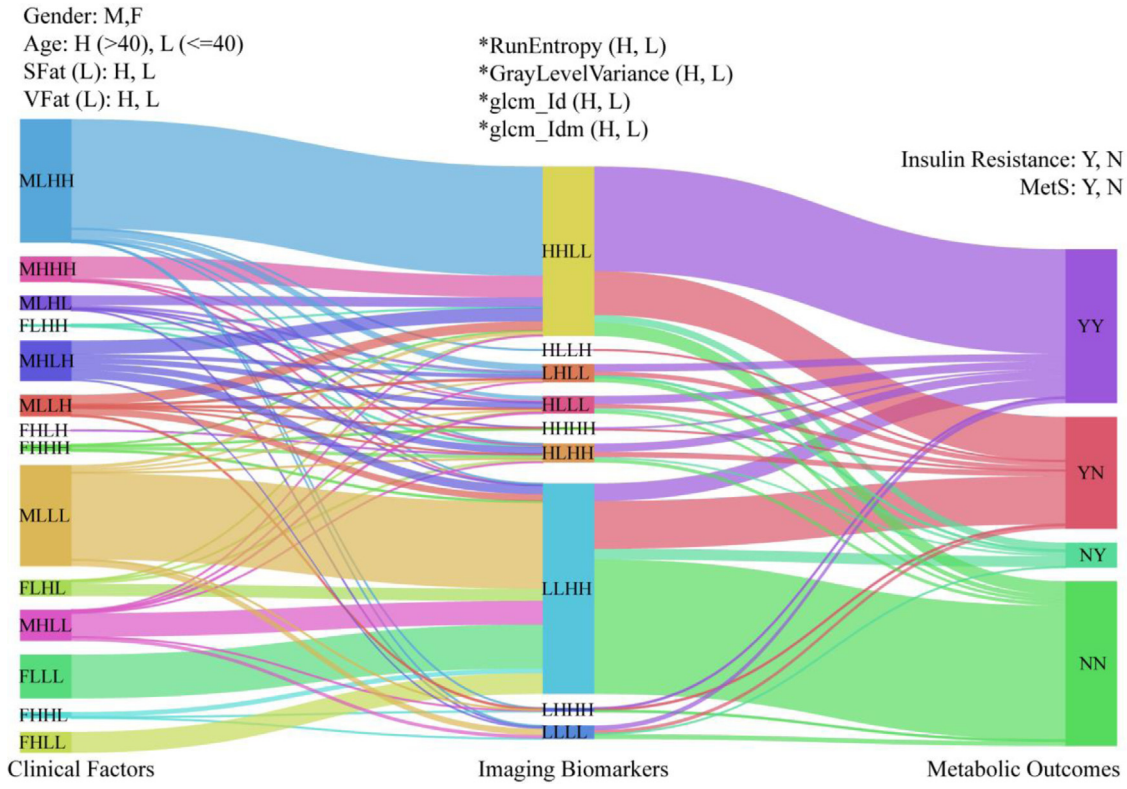

Fig. 4. Correlation among clinical factors, imaging biomarkers, and metabolic outcomes.

Table 3
Students' *t*-test for imaging biomarkers stratified by metabolic-related traits.

Metabolic Traits	State	RunEntropy[a]	GrayLevelVariance[b]	glcm_Id[c]	glcm_Idm[d]
MetS	Yes	2.911±0.118	4.519±0.663	0.595±0.040	0.588±0.050
	No	2.741±0.145	3.779±0.690	0.647±0.048	0.622±0.059
	t	16.633	13.934	15.335	15.115
Central Obesity	Yes	2.890±0.126	4.456±0.681	0.598±0.041	0.561±0.051
	No	2.668±0.098	3.417±0.363	0.675±0.026	0.656±0.031
	t	25.524	25.837	29.876	29.948
Visceral Obesity (Inbody)	Yes	2.907±0.115	4.536±0.658	0.594±0.040	0.556±0.049
	No	2.679±0.105	3.466±0.390	0.669±0.030	0.649±0.036
	t	26.814	26.312	28.216	28.377
Visceral Obesity (FatScan)	Yes	2.872±0.125	4.357±0.679	0.608±0.045	0.573±0.056
	No	2.638±0.102	3.309±0.381	0.676±0.030	0.658±0.036
	t	24.878	25.239	22.680	22.862
Insulin Resistance	Yes	2.880±0.133	4.405±0.711	0.604±0.046	0.569±0.057
	No	2.706±0.133	3.600±0.579	0.658±0.042	0.636±0.052
	t	16.820	16.194	15.895	15.947

all $P < 0.0001$.
[a] Wavelet HHH GLRLM RunEntropy.
[b] GLZSM GrayLevelVariance.
[c] Wavelet LLH glcm Id.
[d] Wavelet LLH glcm Idm.

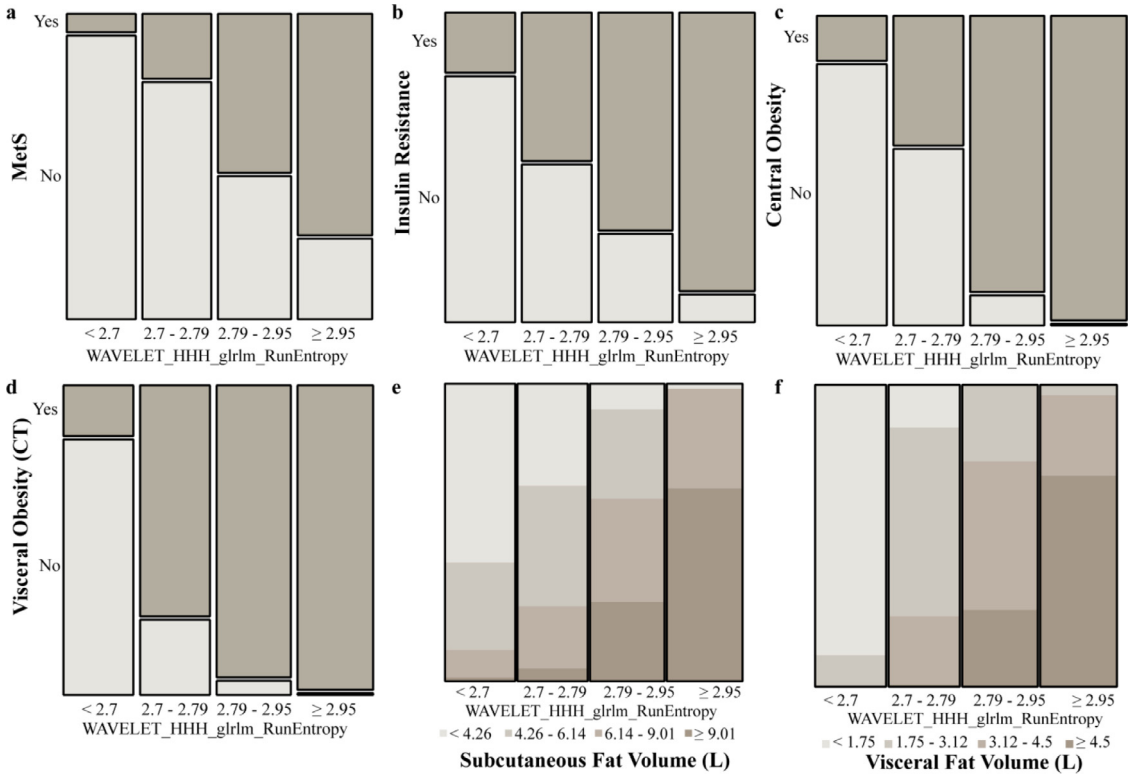

Fig. 5. Correlation between RunEntropy biomarkers and metabolic outcomes.

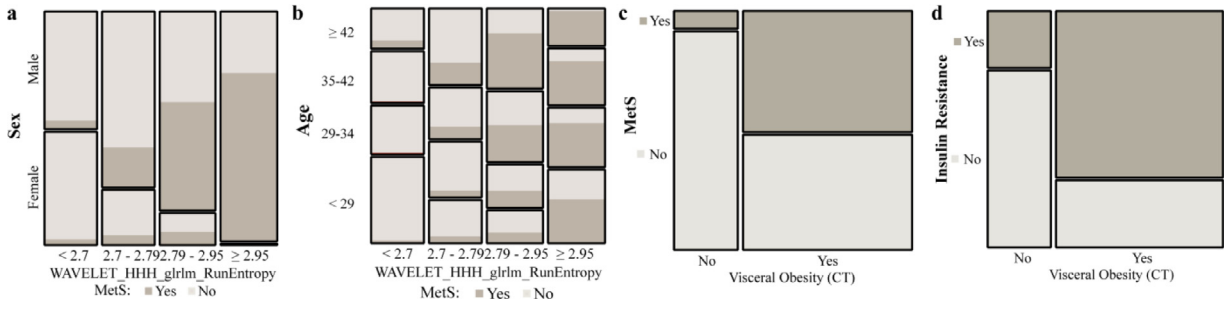

Fig. 6. Correlation between RunEntropy biomarkers and clinical factors (a, b), and relationship between visceral obesity and metabolic outcomes (c, d).

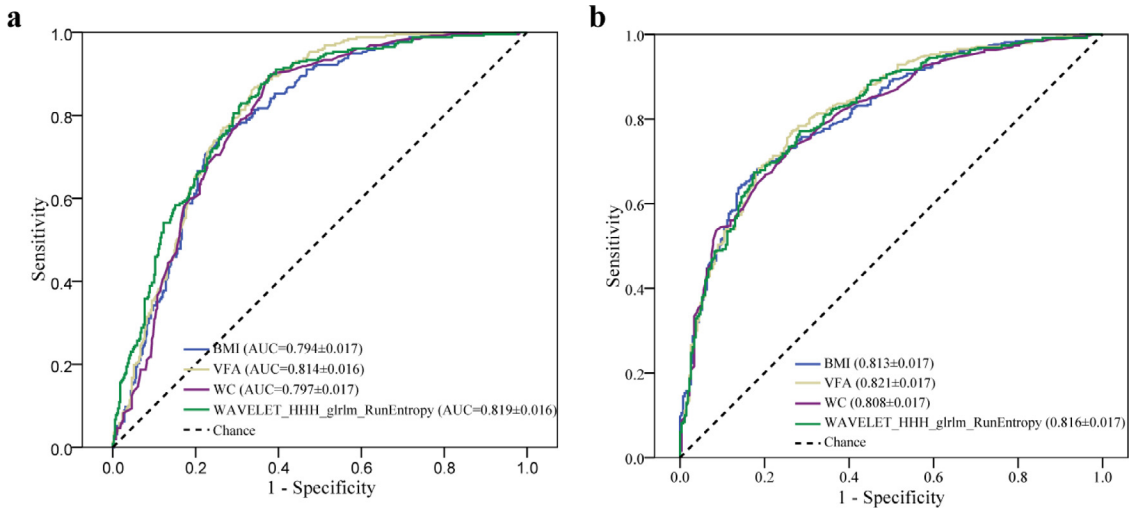

Fig. 7. Performance of *RunEntropy* biomarkers for the diagnosis of MetS (a) and insulin resistance (b).

Table 4
Number of MetS versus Non-MetS cases for follow-up studies and compared to their baseline counterparts.

Studies[a]	State	High	Medium-High	Medium-Low	Low
Baseline	MetS	49	53	17	6
	Non-MetS	16	45	53	99
Follow up	MetS	44	50	19	5
	Non-MetS	21	48	51	100

[a] Number of 338 studies in the MedSV cohort that followed up. RunEntropy subgroups: High, Medium-High, Medium-Low, and low.

Besides, participants with a higher quartile of *RunEntropy* presented with higher BMI, WC, CT-VFA, FPG, 2-h PG, HbA1c, fasting and 2-h serum insulin levels, blood pressure, disturbed lipid profiles, low-grade inflammation, and insulin resistance (ANOVA, $P = 0.012$ for TC, $P < 0.001$ for the other indices). Spearman correlation analysis showed that *RunEntropy* was significantly associated with HOMA-IR ($r = 0.65$, $P < 0.001$) and hs-CRP ($r = 0.46$, $P < 0.001$). After adjusting for age, sex, BMI, and CT-VFA, *RunEntropy* remained significantly correlated with HOMA-IR (multiple linear regression, $P = 0.002$).

3.5. Analysis of follow-up studies with imaging biomarkers

To evaluate the long-term predictive effectiveness of the identified imaging biomarkers, we received a total of 338 follow-up subjects and compared them with their baseline counterparts for MetS status. As shown in Table 4, the *RunEntropy* biomarker is consistently effective for screening out low- and high-risk subjects. For example, a substantial majority of the cases (99 out of 105) classified as *Low-RunEntropy* in baseline still maintained non-MetS status at the end of the 3.5-year follow-up. This finding suggests that chances to develop MetS for people with *Low-RunEntropy* can be as low as 4.8% in following 3.5 years. While, volunteer subjects classified as *High-RunEntropy* in baseline demonstrated significantly (Chi-square test, $P < 0.001$) higher risk (49 out of 65, or 75.4% as MetS in baseline; 44 out of 65, or 67.7% as MetS in follow-up) to develop MetS compared with Low-RunEntropy cases.

3.6. Predicting surgery-induced weight loss effects with imaging biomarkers

The predictive effectiveness of the identified imaging biomarkers was further strengthened in bariatric surgery studies (63 obese patients, median follow-up interval of 13.0 months after surgery). In parallel with the reduction in visceral fat percentage (V-Fat%) and visceral fat area (CT-VFA), the values of three out of the top four imaging markers (except for *GLZSM GrayLevelVariance*) were all significantly decreased after the surgery (Students' *t*-test, all $P < 0.05$) (Table 5).

As shown in Fig 8a,b, the *RunEntropy* biomarker was closely related to the visceral fat percentage ($r = 0.669$; linear regression, $P < 0.001$) and visceral fat area ($r = 0.707$; linear regression, $P < 0.001$) of obese patients before and after surgery. Combined with age and sex, the ten metabolic-related imaging biomarkers obtained before surgery yielded an average AUC of 0.753 and an accuracy of 63.5% for estimation of %EWL category (Fig 8d) in the multinomial logistic regression analysis. Further combined with preoperative fat

Table 5
Paired students' *t*-test for biomarkers before and after bariatric surgery.

Variables	Before Surgery		After Surgery		Paired Differences		*t*	*P* (2-tailed)
	Mean	STD	Mean	STD	Mean	95% Confidence Interval of the Difference		
V-Fat%	13.570	4.261	8.843	3.183	4.726	3.668, 5.784	8.931	< 0.001
CT-VFA	212.953	62.881	104.976	55.134	107.978	93.556, 122.399	14.993	< 0.001
RunEntropy[a]	2.658	0.047	2.534	0.112	0.124	0.095, 0.152	8.636	< 0.001
glcm_Id[b]	0.689	0.070	0.706	0.077	−0.017	−0.031, −0.003	−2.472	0.016
glcm_Idm[c]	0.672	0.084	0.692	0.092	−0.020	−0.036, −0.003	−2.390	0.020
GrayLevelVariance[d]	3.420	0.451	3.426	0.308	−0.006	−0.138, 0.125	−0.096	0.924

Number of paired studies (before and after surgery): 63.
[a] Wavelet HHH GLRLM RunEntropy.
[b] Wavelet LLH glcm Id.
[c] Wavelet LLH glcm Idm.
[d] GLZSM GrayLevelVariance.

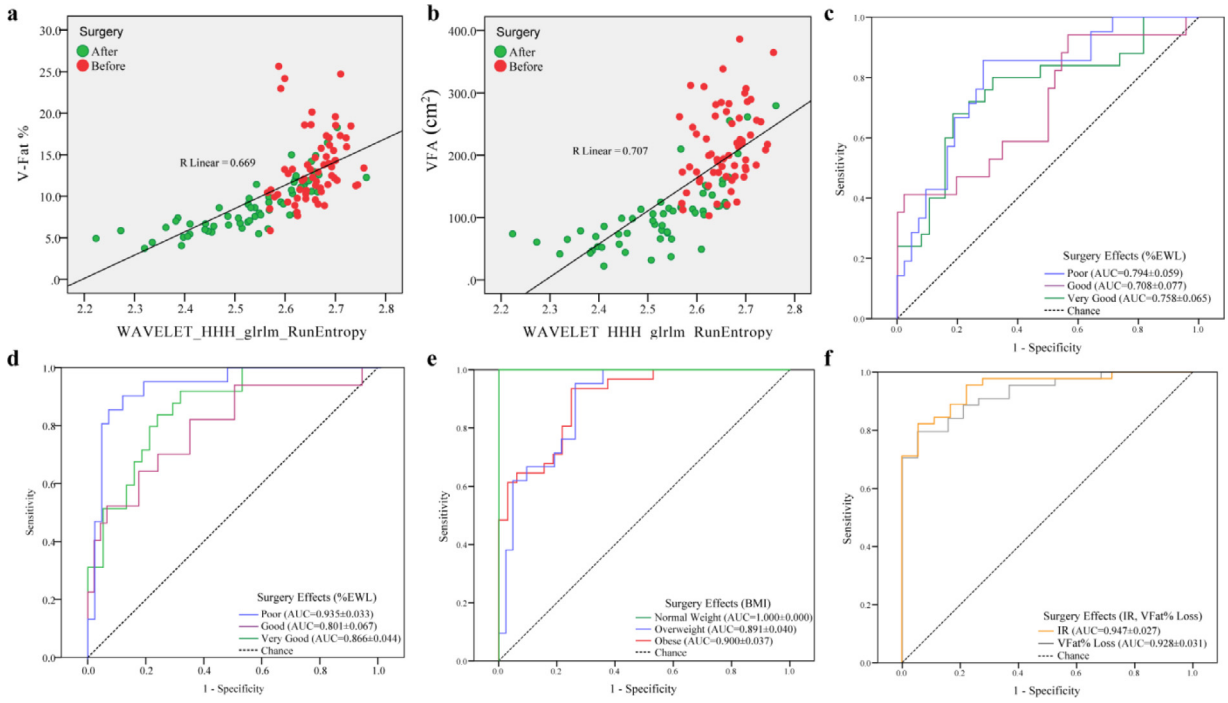

Fig. 8. Imaging biomarkers for estimation of surgery-induced weight loss effects.

percentage and fat area, those VAT texture features obtained from preoperative CT subjects achieved higher performances for predicting %EWL category (average AUC of 0.867, and accuracy of 74.6%), postoperative BMI group (average AUC of 0.930, and accuracy of 76.2%) and other important postoperative outcomes, such as insulin resistance (AUC of 0.947±0.027, and accuracy of 88.9%) and excess visceral fat loss (AUC of 0.928±0.031, and accuracy of 84.1%) (Fig 8d–f). In comparison, the conventional CT features (fat percentage and fat area, combined with age and gender) achieved a much lower performance if not combined with the identified texture imaging biomarkers, for example, average AUC of 0.776 and accuracy of 55.6% for assessment of %EWL category, and average AUC of 0.808 and accuracy of 61.9% for postoperative BMI group (S2 Fig). Consistent results were achieved in S3 Fig where China criteria (overweight: 24.0–27.9 kg/m^2, and obesity is BMI $\geq$ 28 kg/m^2) [35] were used to stratify BMI groups.

4. Discussion

In the present study, texture features extracted from VAT and identified with machine learning were found to be significantly associated with metabolic syndrome and related disorders. Comprising of several imaging biomarkers, the imaging signature provided a more precise classification of the metabolic status and showed good performance for clustering the prevalence of visceral obesity, insulin resistance, and MetS. VAT texture features obtained from the umbilicus level achieved superior predictive performance compared to conventional CT markers, and more importantly, the proposed approach does not require routinely scanning of the upper or entire abdomen, making it less radiation, theoretically more cost-effective, and more viable for application in clinical practice.

Besides noninvasively measuring major metabolic outcomes of volunteer subjects, the proposed method can also provide guidance for bariatric surgery through estimating surgery-induced weight loss effects, including %EWL category, postoperative BMI group, and postoperative insulin resistance, etc. Those important surgery outcomes can be only measured after surgery using existing techniques. In comparison, our method utilized preoperative imaging biomarkers and achieved high predictive performance, which may largely benefit obese patients who are expected to undergo surgery (avoid unnecessary bariatric surgeries for patients that are estimated as low weight loss benefits).

In the 1940s, Vague et al. first raised the concept of central obesity [36], which is more significantly associated with cardiometabolic disorders than peripheral obesity [37]. To date, central obesity has been considered the core trigger of MetS; unfortunately, only quantitative factors, such as the distribution of different fat depots, fat volume, and relative fat percentage, were taken into account to define central obesity. Qualitative factors, such as the texture of fat tissues, however, were not disclosed and linked to the severity of obesity, mainly due to the lack of effective tools. For subjects of the same age and sex, they may differ largely in their cardiometabolic characteristics even if they have similar BMI and body fat distribution, which indicates a metabolic heterogeneity of fat tissues. One of the underlying causes is the abnormal remodeling capacities of visceral fat tissues, which are usually attributed to fibrosis, neovascularization, apoptosis and necrosis of adipocytes, chronic inflammatory infiltration, and even bacterial translocation to visceral adipose tissues due to increased intestinal permeability [17,38]. Our study found that the heterogeneity of VAT texture (fat quality) is significantly related to the prevalence of visceral obesity and MetS in a young or middle-aged Chinese population. The *High-RunEntropy* subgroup exhibited a significantly higher risk of developing MetS than the *Low-RunEntropy* subgroup. Interestingly, *RunEntropy* measures the uncertainty (randomness) in the distribution of run lengths and gray levels, and a higher value of *RunEntropy* indicates more heterogeneity in the tissue texture patterns (VAT tissue in this work) [32]. The unfavorable outcome was observed in a 3.5-year longitudinal follow-up for subjects with high *RunEntropy* at baseline, which indicated that subjects with higher heterogeneity of VAT texture tended to have a higher risk of developing metabolic-related disorders. Thus, the imaging texture biomarkers could be used as a useful measurement approach for fat quality, especially for visceral fat tissues. The diagnostic performance of the *RunEntropy* biomarker on MetS was further compared with routine clinical parameters, including BMI, waist circumference, and visceral fat area, and we found that the imaging biomarker achieved

better predictive power especially for MetS assessment. In addition to MetS and visceral obesity, the imaging biomarker could serve as a risk predictor for insulin resistance. A significant association was also found between *RunEntropy* and hs-CRP, an important indicator of chronic systemic inflammation. These findings highlight the roles of fat quality (adipose tissue texture) in the early physiopathological events of subclinical inflammation and metabolic disorders.

The quality of adipose tissue in relation to metabolic outcomes was also highlighted in the literature. For example, Abdennour et al. reported that diabetic subjects have increased stiffness in their subcutaneous adipose tissue (SAT) [39]. They found that SAT stiffness was associated with tissue fibrosis, obesity, and diabetes-related traits. Their studies on patients with gastric bypass surgery indicated that functional alterations of adipose tissue are associated with the response to surgery-induced weight loss. The study suggested noninvasive evaluation of SAT stiffness might be useful in clinical practice. Chabot K et al. found that obese patients with diabetes had a significantly higher degree of adipose tissue fibrosis [40]. Muir et al. collected adipose tissue biopsies during the bariatric surgery and concluded that the mechanisms of fibrosis are qualitatively different between VAT and SAT, and VAT plays a more important role for metabolic diseases including obesity and diabetes [41]. Given the difficulty in collecting postoperative VAT biopsies due to the invasive operation being involved, it becomes increasingly more important to develop alternative noninvasive measurement methods. As the degrees of fibrosis and stiffness (and other qualities that affect metabolic outcomes) may have been reflected on the texture of adipose tissue and monitored through deciphering CT scans, the underlying mechanism of our method is thus rational and explainable. Future studies are yet expected to explore the texture of adipose tissue in relation to fibrosis, metabolic outcomes, and their association with CT imaging features, especially after bariatric surgeries.

Sleeve gastrectomy has become the most popular procedure worldwide in recent years to help severely obese patients lose weight [42] because the surgery is technically easier to perform and with less morbidity. Thus, it is reasonable to believe that findings under sleeve gastrectomy are considered more representative and applicable. Another most commonly performed bariatric surgery is Roux-en-Y gastric bypass that has similar effects in terms of reducing weights and improving comorbidities, such as T2DM, hypertension, and hyperlipidemia [43]. The common weight-loss mechanism of the two surgical approaches is to reduce appetite and energy intake which results in a reduction of the size of resident adipocytes and thereafter content of fat depots [44]. The mass reduction of visceral adipose tissue/depots (VAT) plays a key role in the metabolic benefits induced by both bariatric surgeries. Existing studies demonstrated that the relative loss of visceral adipose tissue after the abovementioned surgical treatments can be significant in a short period [45–47]. It is a rational hypothesis that the texture changes of VAT are also comparable under different bariatric surgeries. Moreover, because quantitative CT markers (including VFA and VAT volume) are widely applicable for measuring the effectiveness of different types of bariatric surgeries, the findings of qualitative CT texture markers in this study are expected to be useful and applicable for other bariatric surgeries as well. In this study, we proposed a feasible and noninvasive strategy that combined VAT texture features with routine clinical parameters and achieved high predictive performance in estimating bariatric surgery outcomes. This novel strategy may help physicians and patients make scientific and more reliable decisions before surgery.

Approximately 20–30% of obese patients undergoing bariatric surgery experience suboptimal weight loss (%EWL $<$ 50%), which is also consistently observed at our center. The underlying reasons, such as environmental factors, genetic background, feeding behaviours, and psychological characteristics, seemed to be related to long-term outcomes [48]. For example, previous studies reported that female patients and patients without a history of diabetes achieved better weight loss, while monogenic obesity mutation carriers accomplished less weight loss [49]. To obtain a better predictive effect, a comprehensive evaluation of biological, genetic, social, and psychological characteristics might be needed, but it is not easily implemented in clinical practice, at least at present.

Recently, some predictive indices were developed; for example, the Chinese visceral adiposity index (VAI) was proposed to estimate visceral fat volume [50]. VAI is a sex-specific mathematical model derived from age, BMI, TG, and HDL-c, but it is unable to serve as a qualitative tool for the assessment of adipose tissue texture. Another study found that common genetic variants explained 37.3% and 38.5% of the variation in predicted VAT mass in females and males, respectively [37]. However, the requirement of comprehensive genetic testing limits its utility in routine clinical practice. In contrast, the image analysis system developed in this study may serve as a reliable and efficient tool for the assessment of adipose tissue texture considering its noninvasive and low-radiation qualities.

Herein, there are some limitations in this study that we need to acknowledge. First, the study was carried out on Chinese subjects and there are certain racial differences in body fat distribution that may affect metabolic outcomes as reported. Additional multiethnic studies would be beneficial to ensure our work is more widely applicable. Future multiracial studies involving more female participants could be carried out if the relevant resources become available. Second, the cardiometabolic outcomes, such as major cardiovascular events and mortality associated with visceral obesity, were not evaluated in the current study mainly because the subjects enrolled are relatively young, which needs a longer-term follow-up. Third, given the size of the surgery cohort, our method that was carried out on laparoscopic sleeve gastrectomy could be further explored and validated on other types of bariatric surgeries. The study of VAT texture features for the estimation of surgery outcomes merits future investigation.

In conclusion, to the best of our knowledge, this is the first study to identify and decipher CT texture features from human visceral adipose tissue for the evaluation and estimation of visceral obesity, insulin resistance, MetS, and surgery-induced weight loss effects. Future work focusing on broader ethnic groups and larger populations may further improve our understanding of metabolic diseases and related complications.

Declaration of Competing Interest

The authors declare that there are no conflicts of interest.

Acknowledgments

We thank Professor Lu Qi from Tulane University Obesity Research Center for his critical advice on the deep phenotyping study in MedSV cohort. We also thank all participants and health investigators for their involvement and contributions to this study. Funding: This work was supported by the National Key R&D Program of China (2018YFC1313800, 2018YFC1314800), the Outstanding Academic Leader Project of Shanghai Municipal Health Commission (2018BR01), Shanghai Municipal Education Commission-Gaofeng Clinical Medicine Grant Support (20161403), Program of Shanghai Academic/Technology Research Leader (19XD1403200), and grants from National Natural Science Foundation (81822009, 91857205, 81730023, 81870582).

Data sharing statement

Computer code and the dataset used in this study have been released in a public repository (GitHub): http://github.com/guoqingbao/DeepAdipose. The dataset contains extracted imaging features of

675 volunteer studies and 63 obesity patients (with bariatric surgery).

Supplementary materials

Supplementary material associated with this article can be found in the online version at doi:10.1016/j.ebiom.2021.103471.

References

[1] The Lancet Gastroenterology & Hepatology. Obesity: another ongoing pandemic. Lancet Gastroenterol Hepatol 2021;6(6):411.
[2] Collaboration NCDRF. Trends in adult body-mass index in 200 countries from 1975 to 2014: a pooled analysis of 1698 population-based measurement studies with 19.2 million participants. Lancet 2016;387(10026):1377–96.
[3] Keys A, Fidanza F, Karvonen MJ, Kimura N, Taylor HL. Indices of relative weight and obesity. J Chronic Dis 1972;25(6):329–43.
[4] Colditz GA, Willett WC, Rotnitzky A, Manson JE. Weight gain as a risk factor for clinical diabetes mellitus in women. Ann Intern Med 1995;122(7):481–6.
[5] Despres JP, Lemieux I, Prud'homme D. Treatment of obesity: need to focus on high risk abdominally obese patients. BMJ 2001;322(7288):716–20.
[6] Pouliot MC, Despres JP, Lemieux S, Moorjani S, Bouchard C, Tremblay A, et al. Waist circumference and abdominal sagittal diameter: best simple anthropometric indexes of abdominal visceral adipose tissue accumulation and related cardiovascular risk in men and women. Am J Cardiol 1994;73(7):460–8.
[7] Despres JP, Lemieux I, Bergeron J, Pibarot P, Mathieu P, Larose E, et al. Abdominal obesity and the metabolic syndrome: contribution to global cardiometabolic risk. Arterioscler Thromb Vasc Biol 2008;28(6):1039–49.
[8] Despres JP. Is visceral obesity the cause of the metabolic syndrome? Ann Med 2006;38(1):52–63.
[9] Kissebah AH, Vydelingum N, Murray R, Evans DJ, Hartz AJ, Kalkhoff RK, et al. Relation of body fat distribution to metabolic complications of obesity. J Clin Endocrinol Metab 1982;54(2):254–60.
[10] Examination Committee of Criteria for 'Obesity Disease' in J, Japan Society for the Study of O. New criteria for 'obesity disease' in Japan. Circ J 2002;66(11):987–92.
[11] Fang L, Guo F, Zhou L, Stahl R, Grams J. The cell size and distribution of adipocytes from subcutaneous and visceral fat is associated with type 2 diabetes mellitus in humans. Adipocyte 2015;4(4):273–9.
[12] Boutens L, Stienstra R. Adipose tissue macrophages: going off track during obesity. Diabetologia 2016;59(5):879–94.
[13] Ledoux S, Queguiner I, Msika S, Calderari S, Rufat P, Gasc JM, et al. Angiogenesis associated with visceral and subcutaneous adipose tissue in severe human obesity. Diabetes 2008;57(12):3247–57.
[14] Munoz A, Abate N, Chandalia M. Adipose tissue collagen and inflammation in nonobese Asian Indian men. J Clin Endocrinol Metab 2013;98(8):E1360–3.
[15] Sun K, Tordjman J, Clement K, Scherer PE. Fibrosis and adipose tissue dysfunction. Cell Metab 2013;18(4):470–7.
[16] Kraunsoe R, Boushel R, Hansen CN, Schjerling P, Qvortrup K, Stockel M, et al. Mitochondrial respiration in subcutaneous and visceral adipose tissue from patients with morbid obesity. J Physiol 2010;588(Pt 12):2023–32.
[17] Fuster JJ, Ouchi N, Gokce N, Walsh K. Obesity-induced changes in adipose tissue microenvironment and their impact on cardiovascular disease. Circ Res 2016;118(11):1786–807.
[18] Sun K, Kusminski CM, Scherer PE. Adipose tissue remodeling and obesity. J Clin Invest 2011;121(6):2094–101.
[19] Hyun SH, Ahn MS, Koh YW, Lee SJ. A machine-learning approach using pet-based radiomics to predict the histological subtypes of lung cancer. Clin Nucl Med 2019.
[20] Tagliafico AS, Piana M, Schenone D, Lai R, Massone AM, Houssami N. Overview of radiomics in breast cancer diagnosis and prognostication. Breast 2019;49:74–80.
[21] Yip SS, Aerts HJ. Applications and limitations of radiomics. Phys Med Biol 2016;61(13):R150–66.
[22] Lambin P, Rios-Velazquez E, Leijenaar R, Carvalho S, van Stiphout RG, Granton P, et al. Radiomics: extracting more information from medical images using advanced feature analysis. Eur J Cancer 2012;48(4):441–6.
[23] Kim SH, Chung JH, Song SW, Jung WS, Lee YA, Kim HN. Relationship between deep subcutaneous abdominal adipose tissue and metabolic syndrome: a case control study. Diabetol Metab Syndr 2016;8(1):10.
[24] Lu CQ, Wang YC, Meng XP, Zhao HT, Zeng CH, Xu W, et al. Diabetes risk assessment with imaging: a radiomics study of abdominal CT. Eur Radiol 2019;29(5):2233–42.
[25] Adams TD, Davidson LE, Litwin SE, Kim J, Kolotkin RL, Nanjee MN, et al. Weight and metabolic outcomes 12 years after gastric bypass. N Engl J Med 2017;377(12):1143–55.
[26] Nielsen MS, Christensen BJ, Schmidt JB, Taekker L, Holm L, Lunn S, et al. Predictors of weight loss after bariatric surgery-a cross-disciplinary approach combining physiological, social, and psychological measures. Int J Obes 2020 (Lond).
[27] Liu R, Zou Y, Hong J, Cao M, Cui B, Zhang H, et al. Rare loss-of-function variants in NPC1 predispose to human obesity. Diabetes 2017;66(4):935–47.
[28] Expert Panel on Detection E, Treatment of High Blood Cholesterol in A. Executive summary of the third report of the national cholesterol education program (NCEP) expert panel on detection, evaluation, and treatment of high blood cholesterol in adults (adult treatment panel III). JAMA 2001;285(19):2486–97.
[29] Grundy SM, Cleeman JI, Daniels SR, Donato KA, Eckel RH, Franklin BA, et al. Diagnosis and management of the metabolic syndrome: an american heart association/national heart, lung, and blood institute scientific statement. Circulation 2005;112(17):2735–52.
[30] Stefan N, Haring HU, Hu FB, Schulze MB. Metabolically healthy obesity: epidemiology, mechanisms, and clinical implications. Lancet Diabetes Endocrinol 2013;1(2):152–62.
[31] Reinhold RB. Critical analysis of long term weight loss following gastric bypass. Surg Gynecol Obstet 1982;155(3):385–94.
[32] van Griethuysen J, Fedorov A, Parmar C, Hosny A, Aucoin N, Narayan V, et al. Computational radiomics system to decode the radiographic phenotype. Cancer Res 2017;77:e104–e7.
[33] Sanasam R, Murthy H, Gonsalves T. Feature selection for text classification based on gini coefficient of inequality. J Mach Learn Res Proc Track 2010;10:76–85.
[34] He K, Zhang X, Ren S, Sun J. Delving deep into rectifiers: surpassing human-level performance on imagenet classification. In: Proceedings of the IEEE international conference on computer vision; 2015.
[35] Wu Y. Overweight and obesity in China. BMJ 2006;333(7564):362–3.
[36] Vague J. Sexual differentiation. a determinant factor of the forms of obesity. 1947. Obes Res 1996;4(2):201–3.
[37] Karlsson T, Rask-Andersen M, Pan G, Hoglund J, Wadelius C, Ek WE, et al. Contribution of genetics to visceral adiposity and its relation to cardiovascular and metabolic disease. Nat Med 2019;25(9):1390–5.
[38] Massier L, Chakaroun R, Tabei S, Crane A, Didt KD, Fallmann J, et al. Adipose tissue derived bacteria are associated with inflammation in obesity and type 2 diabetes. Gut 2020;69:1796–806. doi: 10.1136/gutjnl-2019-320118.
[39] Abdennour M, Reggio S, Le Naour G, Liu Y, Poitou C, Aron-Wisnewsky J, et al. Association of adipose tissue and liver fibrosis with tissue stiffness in morbid obesity: links with diabetes and bmi loss after gastric bypass. J Clin Endocrinol Metab 2014;99(3):898–907.
[40] Chabot K, Gauthier MS, Garneau PY, Rabasa-Lhoret R. Evolution of subcutaneous adipose tissue fibrosis after bariatric surgery. Diabetes Metab 2017;43(2):125–33.
[41] Muir LA, Neeley CK, Meyer KA, Baker NA, Brosius AM, Washabaugh AR, et al. Adipose tissue fibrosis, hypertrophy, and hyperplasia: correlations with diabetes in human obesity. Obesity 2016;24(3):597–605 (Silver Spring).
[42] Ozsoy Z, Demir E. Which bariatric procedure is the most popular in the world? A bibliometric comparison. Obes Surg 2018;28(8):2339–52.
[43] Shoar S, Saber AA. Long-term and midterm outcomes of laparoscopic sleeve gastrectomy versus Roux-en-Y gastric bypass: a systematic review and meta-analysis of comparative studies. Surg Obes Relat Dis 2017;13(2):170–80.
[44] Miras AD, le Roux CW. Mechanisms underlying weight loss after bariatric surgery. Nat Rev Gastroenterol Hepatol 2013;10(10):575–84.
[45] Weiss R, Appelbaum L, Schweiger C, Matot I, Constantini N, Idan A, et al. Short-Term dynamics and metabolic impact of abdominal fat depots after bariatric surgery. Diabetes Care 2009;32(10):1910.
[46] Galanakis CG, Daskalakis M, Manios A, Xyda A, Karantanas AH, Melissas J. Computed tomography-based assessment of abdominal adiposity changes and their impact on metabolic alterations following bariatric surgery. World J Surg 2015;39(2):417–23.
[47] Miller GD, Carr JJ, Fernandez AZ. Regional fat changes following weight reduction from laparoscopic Roux-en-Y gastric bypass surgery. Diabetes Obes Metab 2011;13(2):189–92.
[48] Sarwer DB, Allison KC, Wadden TA, Ashare R, Spitzer JC, McCuen-Wurst C, et al. Psychopathology, disordered eating, and impulsivity as predictors of outcomes of bariatric surgery. Surg Obes Relat Dis 2019;15(4):650–5.
[49] Li Y, Zhang H, Tu Y, Wang C, Di J, Yu H, et al. Monogenic obesity mutations lead to less weight loss after bariatric surgery: a 6-year follow-up study. Obes Surg 2019;29(4):1169–73.
[50] Xia MF, Chen Y, Lin HD, Ma H, Li XM, Aleteng Q, et al. A indicator of visceral adipose dysfunction to evaluate metabolic health in adult. Chinese Sci Rep 2016;6:38214.